Patterning and Conductivity Modulation of Conductive Polymers by UV Light Exposure

Edberg, Jesper; Iandolo, Donata; Brooke, Robert; Liu, Xianjie; Musumeci, Chiara; Andreasen, Jens Wenzel; Simon, Daniel T.; Evans, Drew; Engquist, Isak; Berggren, Magnus

Published in:
Advanced Functional Materials

Link to article, DOI:
10.1002/adfm.201601794

Publication date:
2016

Document Version
Peer reviewed version

Patterning and Conductivity Modulation of Conductive Polymers by UV Light Exposure

Jesper Edberg, Donata Iandolo, Robert Brooke, Xianjie Liu, Chiara Musumeci, Jens Wenzel Andreasen, Daniel Simon, Drew Evans, Isak Engquist and Magnus Berggren

Journal Article

Original Publication:

Jesper Edberg, Donata Iandolo, Robert Brooke, Xianjie Liu, Chiara Musumeci, Jens Wenzel Andreasen, Daniel Simon, Drew Evans, Isak Engquist and Magnus Berggren, Patterning and Conductivity Modulation of Conductive Polymers by UV Light Exposure, Advanced Functional Materials, 2016. 26(38), pp.6950-6960.
http://dx.doi.org/10.1002/adfm.201601794

Patterning and Conductivity Modulation of Conductive Polymers by UV Light Exposure

Jesper Edberg[a], Donata Iandolo[a], Robert Brooke[a], Xianjie Liu[b], Chiara Musumeci[b], Jens Wenzel Andreasen[c], Daniel T. Simon[a], Drew Evans[d], Isak Engquist[a*] and Magnus Berggren[a]

*Corresponding author: isak.engquist@liu.se

[a]Linköping University

Department of Science and Technology, Laboratory of Organic Electronics

SE-601 74 Norrköping, Sweden

[b]Linköping University

Department of Physics, Chemistry and Biology

SE-581 83 Linköping, Sweden

[c]Technical University of Denmark

Department of Energy Conversion and Storage

4000 Roskilde, Denmark

[d]University of South Australia

Future Industries Institute

5001 Adelaide, Australia

Abstract

We demonstrate a novel patterning technique of conductive polymers produced by vapor phase polymerization. The method involves exposing an oxidant film to UV light which changes the local chemical environment of the oxidant and subsequently the polymerization kinetics. This procedure is used to control the conductivity in the conjugated polymer poly(3,4-ethylenedioxythiophene):tosylate (PEDOT:Tos) by more than 6 orders of magnitude in addition to producing high resolution patterns and optical gradients. We investigate the mechanism behind the modulation in the polymerization kinetics by UV light irradiation as well as the properties of the resulting polymer.

1. INTRODUCTION

The development of highly conductive polymers has been one of the major goals for organic electronics. Recently, conductivity of 3400 S/cm was demonstrated for vapor phase polymerized (VPP) poly(3,4-ethylenedioxythiophene):tosylate (PEDOT:Tos) thin films[1] and 7600 S/cm for VPP PEDOT:Cl single-crystal nanowires[2], rivaling ITO as the material of choice for transparent flexible electrodes. Development of patterning techniques for organic materials is another vein of research receiving a large amount of attention. These patterning techniques include laser cutting[3], ink jet printing[4], screen printing[5], transfer printing[6] and photolithography[7-11]. Each of these methods has its respective advantages and disadvantages.

Direct writing methods including laser cutting and inkjet printing are typically limited in resolution to approximately 10-100 μm. With contact transfer techniques, such as mold transfer printing[6] and dip pen nanolithography[12], it is possible to achieve sub-micrometer resolution. However, mold transfer printing suffers from deformation of the flexible mold and dip pen nanolithography is slow in patterning and therefore not suitable for large area production. Photolithography is one of the most established and well-studied micro fabrication methods owing to its high resolution, reliability and high throughput. However, conventional photolithography involves many manufacturing steps and the use of solvents which are often damaging to the organic material to be patterned. To avoid these problems, different approaches have been explored such as reduced number of manufacturing steps[8], new (less harmful) solvents[9], protective layers and dry liftoff techniques.[11]

Jeonghun et al. reported a method to modify the conductivity of PEDOT films by a UV-initiated crosslinking of chemically modified EDOT.[13] By using a mask they were able to pattern the polymer with sub-micrometer linewidth. The conductivity was varied between 120 S/cm (unexposed) and 1.7 mS/cm (exposed). Tehrani et al. used electrochemical overoxidation

as a patterning technique for PEDOT and they were able to achieve a 7 orders of magnitude difference in conductivity between exposed and non-exposed regions.[14]

In this work we report a new method of patterning vapor phase polymerized PEDOT:Tos using UV light. Similar to the work by Kim[13] and Tehrani et al.[14], it involves a spatially controlled reduction in conductivity. However, the technique reported herein differs from previous studies in the exposure of the oxidant prior to polymerization resulting in a reduction in the polymer conductivity. We investigate the effect of UV light on the oxidant as well as the origin of the reduction in conductivity and explore how this effect can be used as a high resolution patterning technique with unique functionality and many advantages over existing patterning methods.

2. EXPERIMENTAL SECTION

2.1 *Materials*

Clevios™ CB 40 V2 (40% wt/wt Fe(III) p-toluenesulfonate (Tosylate) in butanol) was purchased from Heraeus (Germany). 3,4-Ethylenedioxythiophene (EDOT) monomer (142.18 g/mol), and the triblock copolymer poly(ethylene glycol)-block-poly(propylene glycol)-block-poly(ethylene glycol) (PEG-PPG-PEG, 5800 g/mol) were purchased from Sigma-Aldrich. All chemicals were used as received without further purification.

2.2 *UV light patterning and vapor phase polymerization of PEDOT:Tosylate*

PEDOT:Tosylate was synthesized by vapor phase polymerization (VPP) by exposing a solution containing Fe(III):Tosylate (the oxidant solution) to EDOT vapor in a vacuum chamber. The oxidant solution was prepared by mixing 2 g of Clevios™ CB 40 V2, 3 g of ethanol (99.7% concentration) and 1.5 g of the triblock copolymer PEG-PPG-PEG 5800 Da (PPP, P123). The resulting solution contains 12.3 wt% Fe(III):Tos and 23.1 wt% PEG-PPG-PEG. Films were obtained by spin coating the oxidant solution at 1500 rpm for 30 s onto glass

substrates with or without four probe electrodes for electrical characterization. The as spun films were baked for 30 s at 70 °C and then kept at 40 °C. Oxidant films were exposed to UV light for different time intervals using a UV lamp with an intensity of 20 mW/cm^2 at 405 nm and 10 mW/cm^2 at 365 nm. VPP was performed under vacuum in a desiccator positioned on a hotplate previously set at 50 °C. EDOT was deposited onto glass substrates at the bottom of the desiccator to ensure EDOT vaporization. After 30 minutes the samples were removed from the desiccator and baked on a hotplate for 2 minutes at 70 °C. The samples were then washed in ethanol (70% concentration) to remove unreacted oxidant solution followed by drying with nitrogen.

2.3 *FTIR*

FTIR measurements were performed using an Equinox 55 spectrometer (Bruker). FTIR spectra were acquired in transmission mode using a resolution of 4 cm^{-1} and 64 scans. Spectra were baseline corrected and smoothed. FTIR analyses were performed on films of CB40, the triblock copolymer, the oxidant solution and of PEDOT:Tosylate deposited onto un-doped SiO_2 wafers.

2.4 *UV-Vis spectroscopy*

Absorption measurements were performed using a Lambda 900 spectrometer (PerkinElmer). Films of the oxidant solution were deposited on glass substrates using the same protocol as reported in section 2.2, and exposed to UV light for different time intervals before running the polymerization procedure. Spectra were recorded between 350-2000 nm.

2.5 *XPS and UPS*

Photoemission experiments were performed using a Scienta ESCA 200 spectrometer in ultrahigh vacuum with a base pressure of 10^{-10} mbar. The measurement chamber was equipped with a monochromatic Al Kα X-ray source providing photons with 1486.6 eV for XPS (X-ray photoemission spectroscopy) and a standard He-discharge lamp with HeI 21.22 eV for UPS

(ultraviolet photoemission spectroscopy). The XPS experimental condition was set so that the full width at half maximum of the clean Au 4f7/2 line was 0.65 eV. The total energy resolution of the UPS measurement was ~80 meV as extracted from the width of the Fermi level of clean gold foil. All spectra were measured at a photoelectron takeoff angle of 0° (normal emission). The work functions of the films were extracted from the determination of the high binding-energy cutoff of the UPS spectra by applying a bias of -3 V to the sample.

2.6 *Atomic force microscopy*

Atomic force microscope (AFM) images were performed in tapping mode using a Veeco Dimension 3100. The morphological images were analyzed using the software WSxM 4.0. Conductive atomic force microscopy (C-AFM) was carried out in a Dimension 3100 microscope (Veeco, Bruker) with a Nanoscope IVa controller, equipped with a conductive-AFM module (1 nA/V current sensitivity). Commercial Pt/Cr coated silicon cantilevers with a spring constant of 0.2 N/m were used to simultaneously acquire topography images and current maps in contact mode by applying a constant load force of 2-5 nN. For the electrical characterization the tip was always kept at ground and a variable DC bias was applied to the gold bottom substrate. All the measurements were performed in ambient atmosphere.

2.7 *GIWAXS*

Grazing Incidence Wide Angle X-ray Scattering analysis was carried out on PEDOT films deposited on silicon wafers. The measurements were performed using a dedicated GIWAXS setup, described by Apitz et al.[15], using a rotating Cu anode as X-ray source, collimated and monochromatized by a multilayer mirror (wavelength 1.5418 Å). The substrates were aligned to an incidence angle of 0.18°, below the critical angle for total reflection for the silicon wafer, and the scattered data were recorded on photostimulable imaging plates.

2.8 *Conductivity*

Gold electrodes in a four-probe configuration were patterned onto glass substrates using thermal evaporation. The area between the inner electrodes was 1x1 cm^2. Polymer films were produced on top of the electrodes using the procedure described in section 2.2. The sheet resistance (R_s) of the samples was measured using a source meter (Keithley 2400) in four-wire sense mode. The conductivity (σ) was calculated using the equation $\sigma = \frac{1}{R_s t}$ where t is the sample thickness. The films thickness was measured using a surface profilometer (Dektak3ST Veeco).

2.9 *Impedance spectroscopy*

The impedance spectra of the polymer samples were measured in a 2-probe setup on an Alpha High Resolution Dielectric Analyzer (Novocontrol) from 100 mHz to 100 kHz with 100 mV AC voltage. Samples with metal electrodes were prepared in the same manner as described in section 2.9.

3. RESULTS

3.1 *Patterning PEDOT:Tos*

Poly(3,4-ethylenedioxythiphene):tosylate (abbreviated PEDOT:Tos) was produced using the vapor phase polymerization (VPP) technique. The process together with the recipe of the oxidant solution outlined in the experimental section was adapted from Fabretto et al.[1] This procedure typically results in polymer films with conductivity >1000 S/cm. By exposing samples to UV light prior to the polymerization step it is possible to dramatically change the optical, electrical and structural properties of the resulting polymer film. Upon exposure of the samples to UV light, the color of the resulting polymer changes from blue to gray, the conductivity is reduced and the surface topography gets rougher. These effects are described

in detail in sections 3.2, 3.4 and the supplementary information. By employing a photomask during the exposure step it is possible to produce a pattern of exposed and unexposed regions on the resultant polymer film. Fig. 1a depicts the UV patterning process where (1) films of an oxidant solution are prepared, (2) the samples are exposed to UV light through a photomask, (3) the samples are exposed to EDOT vapors in a closed chamber where the polymerization takes place and (4) the samples are baked on a hotplate at 70 °C followed by rinsing in ethanol. This procedure is described in greater detail in section 2.2. Fig. 1b shows how an image can be transferred to the polymer using a mask manufactured in an office printer while Fig. 1c-1e show PEDOT patterns on glass substrates made with a quartz photomask with chromium patterns. Fig. 1c shows a circuit structure where the smallest feature is 10 µm. (A layer of gold was added to the substrate to give better contrast in the optical microscope.)

After the polymerization the color difference between the polymer of the masked and exposed regions are clearly visible. However, upon placing the sample on a hotplate (post-polymerization baking step) the color of both regions changes to a darker shade within seconds. The nature of this phenomenon is discussed in detail in section 4.2. The mechanical properties of the film in the regions that were exposed to UV differ dramatically whether the baking step is performed or not. After the baking step it is possible to rinse the whole film with ethanol without any degradation of any region. However, when omitting the baking step, the polymer in the exposed regions is completely dissolved in the washing step, leaving only the pattern of the masked areas intact. Fig. 1d and 1e show two samples with PEDOT patterns where one of the samples (Fig. 1e) was washed without the post-polymerization baking step while the other sample (Fig. 1d) was baked before washing. An additional example of baked and unbaked samples of patterned samples with smaller features are shown in Fig. S1. In Fig. 1e, the exposed regions have been stripped away while the exposed polymer remains in Fig. 1d. The process of removing the exposed polymer is shown in Fig. S2.

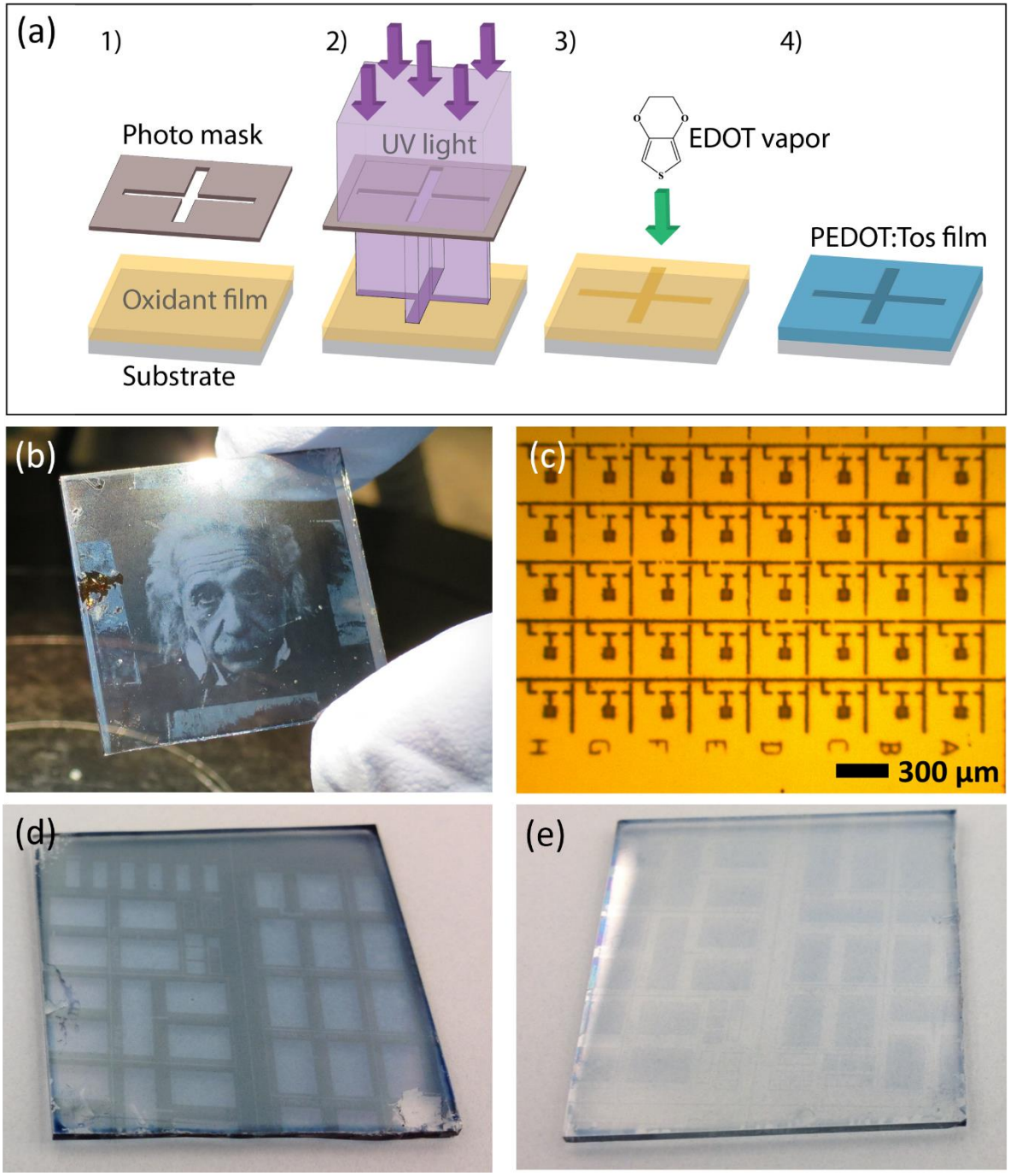

Figure 1. Patterning of VPP PEDOT:Tos. (a) The patterning procedure, (b) an example of a complex image patterned in the polymer, (c) electronic circuit patterned on Au substrate with minimum linewidth of 10 µm, line pattern on Au with (d) and without (e) the post polymerization baking step.

3.2 *Conductivity and patterning resolution*

The in-plane conductivity of the PEDOT:Tos films was investigated as a function of UV exposure time (Fig. 2). Oxidant films deposited on glass substrates carrying four-probe metal electrodes were exposed for increasing time lapses (0, 30, 60, 120, 300 and 600 s) prior to polymerization. Three such samples were fabricated for each exposure time. The resulting conductivity values are shown in Fig. 2a. Data was fitted by an exponential function (Eq. (1)) where σ is the conductivity and t is the exposure time. This equation can be used to calculate the exposure time when a particular conductivity is desired.

Fig. 2a also shows two data points related to polymer samples that were kept in the polymerization chamber for an extended period of time (15 h), but were not baked before washing. These samples did not dissolve during the washing step. The longer polymerization time seems thus to increase the structural integrity of the exposed polymer samples.

$$\sigma = 61e^{-t/32} + 956e^{-t/12} + 2 \cdot 10^{-4} \quad \text{[S/cm]} \qquad (1)$$

The influence played by the amount of the triblock copolymer (PEG-PPG-PEG) in the oxidant solution on the patterning process was investigated. Fig. 2b shows the conductivity of unexposed and exposed samples as well as the conductivity ratio as a function of the weight percentage of the copolymer. The conductivity ratio is defined as the ratio between the conductivity of the unexposed sample and the conductivity of the exposed sample at a specific block copolymer weight percentage. It can be seen that the conductivity ratio increases exponentially with the amount of the copolymer up to ~23 wt%. After this point phase separation becomes visible in the samples and the conductivity ratio decreases. The thickness of the polymer samples increases linearly with increasing UV light exposure time. This can be seen both for samples that are polymerized for a short time and followed by baking as well as for samples that are polymerized for a long time without baking (Fig. 2c). The statistics of the

“30 minutes’ polymerization” samples were done with three samples for each exposure time and with five samples for each exposure time for the “15 hours’ polymerization” samples. The increase in films thicknesses could be explained with increased reaction kinetics in the UV-treated oxidant films. Samples that were polymerized for 15 hours were 75-175 nm thicker than films obtained with the 30 minutes’ polymerization. This could explain why the samples that were polymerized for increased periods survived the washing step when omitting the baking step. Fig 2d shows the average height- and current profile from Conductive AFM (C-AFM) measurements on a 20 µm wide patterned line. The line (shown in Fig. 2f) was patterned on glass substrate without removing the exposed regions. The measurement was performed by scanning the tip across the width of the line (as indicated by the arrow in Fig. 2f) while measuring the current along the line. In Fig. 2d, the line is centered at 30 µm where the current is peaking. It is also clear that the average height is larger in the exposed regions outside the line as was shown in Fig. 2c. The edge of the line displays a gradient both in the height and current. This gradient, which is ~7 µm wide, can clearly be seen in the patterns of Fig. 2e and 2f. As can be seen in Fig. 2e, all patterns smaller than ~14 µm will be affected by this gradient, in its entirety. The gradient is most likely caused by light-leakage under the pattern of the mask during UV exposure; an artifact caused by the space between the mask and the substrate. The width of the gradient is on the same order as the distance between the mask and the substrate (~10 µm). Putting the mask in contact with the substrate might improve the resolution. However, this is not possible with the current recipe of the oxidant solution which makes the substrate stick to the mask.

To further investigate the gradient, C-AFM measurements were performed in the out-of-plane direction of patterned lines on gold substrate. Fig. S4 shows the measurement on 10, 20, 50 and 100 µm lines. By measuring the current in the out-of-plane direction of the polymer there is no need to correct for the dimensions of the lines. Although the peak current values vary for

the different lines, the ratio between the current in the middle of the line (the peak current) and the current outside the line is on the same order (~100) for the 20, 50 and 100 µm lines while this ratio is much smaller for the 10 µm line (~10). This observation shows that the conductivity of the gradient area is considerably smaller than that of the polymer in the regions that were completely protected from UV light. This result represents a limit to the resolution. The current-ratio in these measurements does not reflect the conductivity ratio of exposed and unexposed regions in the plane of the polymer since the cross-plane and out-of-plane conductivity of PEDOT often differ by several orders of magnitude, as previously reported.[16]

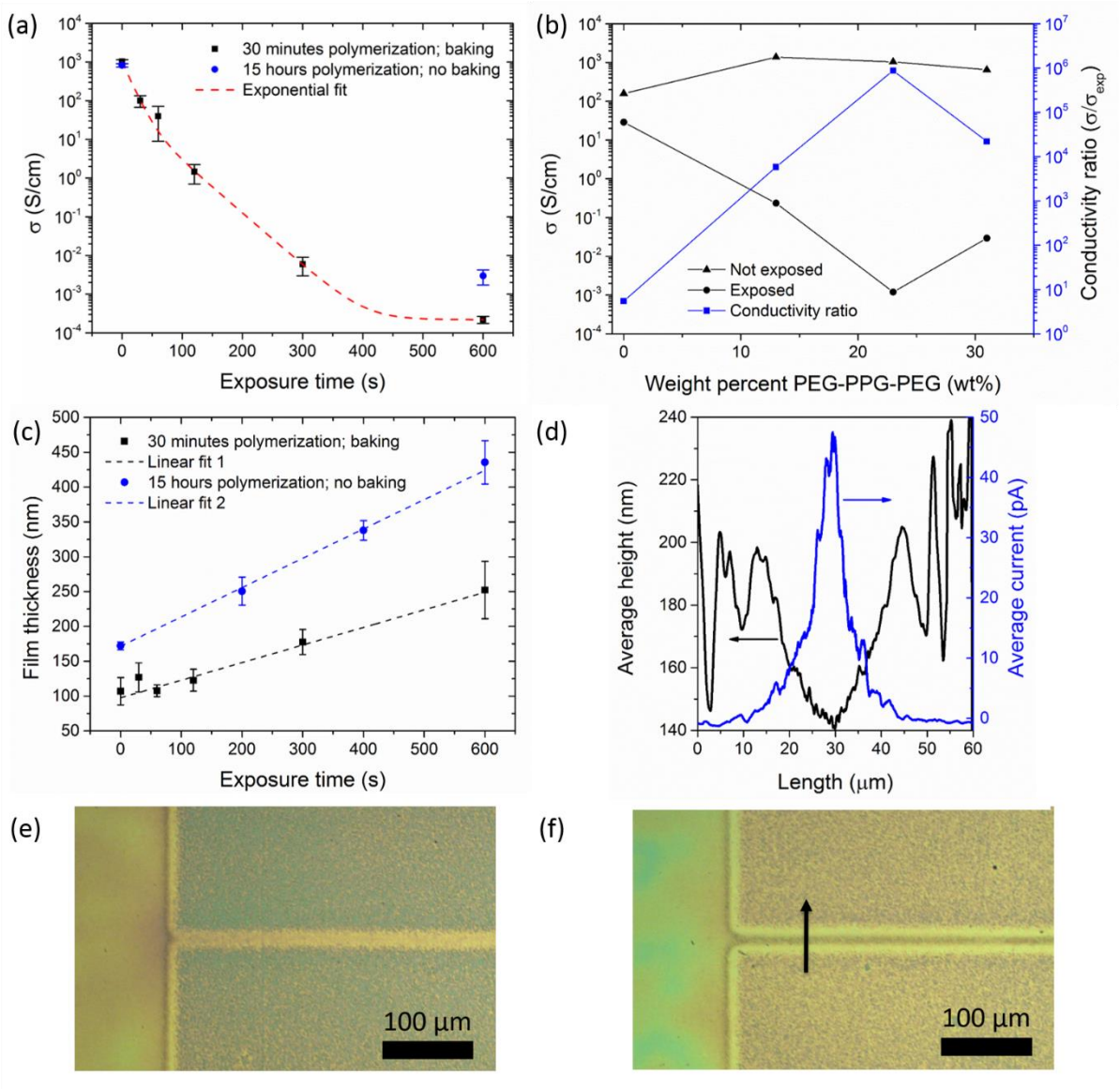

Figure 2. Conductivity of polymer films as a function of (a) exposure time and (b) weight percentage (wt%) of PEG-PPG-PEG in the oxidant solution. (c) Film thickness as a function of exposure time, (d) C-AFM measurement over a 20 µm wide patterned line, (e and f) microscope images of a 10 µm (e) and 20 µm (f) patterned lines. The arrow in (f) indicates the C-AFM scanning direction.

3.3 *FTIR spectroscopy*

Films of Clevios CB40, the triblock copolymer and the oxidant solutions were analyzed in transmission mode (Figure 3). Films prepared from the oxidant solution displays the typical peaks of both $Fe(Tos)_3$ and triblock copolymer, although it differs from the spectrum of the pure $Fe(Tos)_3$ crystals as previously showed by Laforgue.[17] Films of Clevios CB40 show a broad band at 3115 cm^{-1} corresponding to H-bonded O-H groups.

When comparing the FTIR spectra for the exposed and unexposed samples, CB40 films show a remarkable change with a clear peak appearing at about 3400 cm^{-1} (Fig. 3a), possibly corresponding to free OH groups (H-bonded OH appearing at 3115 cm^{-1}). $Fe(Tos)_3$ is known to exhibit a broad peak close to 3400 cm^{-1} in its hydrated form (hexahydrate) which does not appear in its anhydrous form.[18] Upon UV exposure, films of CB40 display several changes in the area between 1670 cm^{-1} and 1645 cm^{-1} (attributable to tosylate CH), the peaks at 1126 cm^{-1} (corresponding to the asymmetric sulfonate stretching vibration), at 684 cm^{-1} (SO stretching) and at 569 cm^{-1} (vibration of C-S bond) become larger. The increase in intensity may suggest an increased degree of freedom for the S and O atoms to vibrate. When analyzing FTIR spectra of both untreated and UV light exposed PPP films, no meaningful differences were detected (Fig. 3c). As it is possible to observe in Fig. 3b, films of the oxidant solution show three main changes in their FTIR profile upon exposure to UV light: the appearance of the peak at 3400 cm^{-1} (free OH groups), the reduction of the intensity of the broad peak at 3142 cm^{-1} (H-bonded OH groups) and the sharpening of the peak at 1647 cm^{-1} (tosylate CH).

FTIR analysis was also performed on PEDOT:Tos films obtained with or without UV light exposure. The main differences between the two sets of data in the FTIR spectra (Fig. 3d) are in three main areas: above 2000 cm^{-1}, between 2970 and 2870 cm^{-1} and at 1510 cm^{-1}. In the area above 2000 cm^{-1}, the electronic absorption from free charge carriers created from the polymerization reaction are localized.[19] As reported earlier by Kvarnstrom et al., upon increasing polymer oxidation level, an increase in the absorption at 4000 and 1500 cm^{-1} is recorded.[20] The area between 2970 and 2870 cm^{-1} is associated with C-C-H stretching modes, whereas the signal at 1510 cm^{-1} corresponds to the C=C stretching mode. The appearance of the peaks between 2970 and 2870 cm^{-1} in addition to the dramatic reduction of the peak at 1510 cm^{-1} may account for shorter polymeric chains. Im and Gleason previously reported that the reduction to almost undetectable levels of the 1510 cm^{-1} peak is associated with shorter PEDOT chains due to the polymerization process.[21]

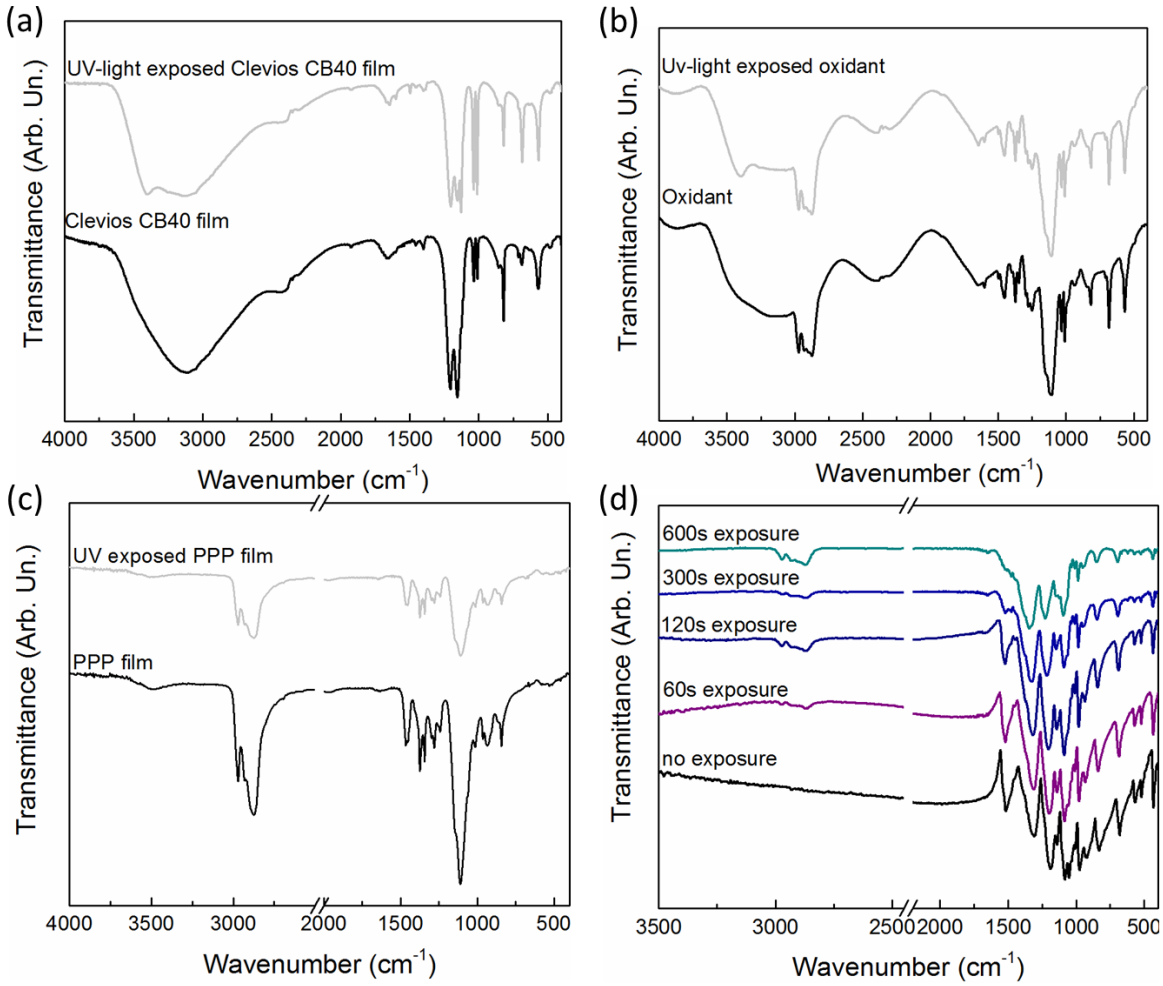

Figure 3. FTIR spectra of (a) Clevios CB 40, (b) oxidant solution, (c) triblock copolymer both exposed and unexposed and (d) PEDOT:Tos for different UV light exposure times.

3.4 *Absorption spectroscopy*

UV-Vis-NIR absorption spectra were acquired in the spectral range 350-2000 nm. Measurements were run on samples that had been exposed to UV light for 60, 120, 300 and 600 seconds, as well as on reference samples that were not exposed (0 s UV). Fig. 4a shows the average spectra for each exposure time and Fig. 4b-4f show the deconvolution of the spectra for each exposure time. Fig. S5 shows the same graph as Fig. 4a but with error bars. The

deconvolution was performed using Gaussian functions.[22] Four peaks were identified in the deconvolution of the absorption spectra. Bubnova et al. described the band transition corresponding to each peak.[23] According to their picture (reproduced in Fig. S6), peak 1 corresponds to an excitation of the neutral polymer (transition *i*), peak 2 comes from to either a transition from the lower polaron level to the higher polaron level (transition *ii*) or from the HOMO level to the higher bipolaron band (transition *iv*), peak 3 is due to to an excitation from the HOMO level to the lower polaron level (transition *iii*) and peak 4 correspond to an excitation from the HOMO level to the lower bipolaron band (transition *v*). Peak 1 grows stronger in relative intensity with increasing times of exposure to UV light. Namely the absorption of neutral PEDOT:Tos usually appears around 600 nm and the shift towards higher energies could be an indication of a shortening of the polymer chains. Peak 2-4 all involve transitions to, or between, polaronic and bipolaronic bands. In untreated PEDOT:Tos bipolarons are the major charge carriers. With increasing exposure times, we can see that the transition associated with bipolarons (peak 4) become weaker in relative amplitude, whereas the transitions associated with polarons (peak 3) become stronger. Peak 2 could be interpreted as a mix between the aforementioned transitions. In the reference samples, peak 2 is centered above 800 nm but, with increasing exposure times, it is shifted to lower wavelengths.

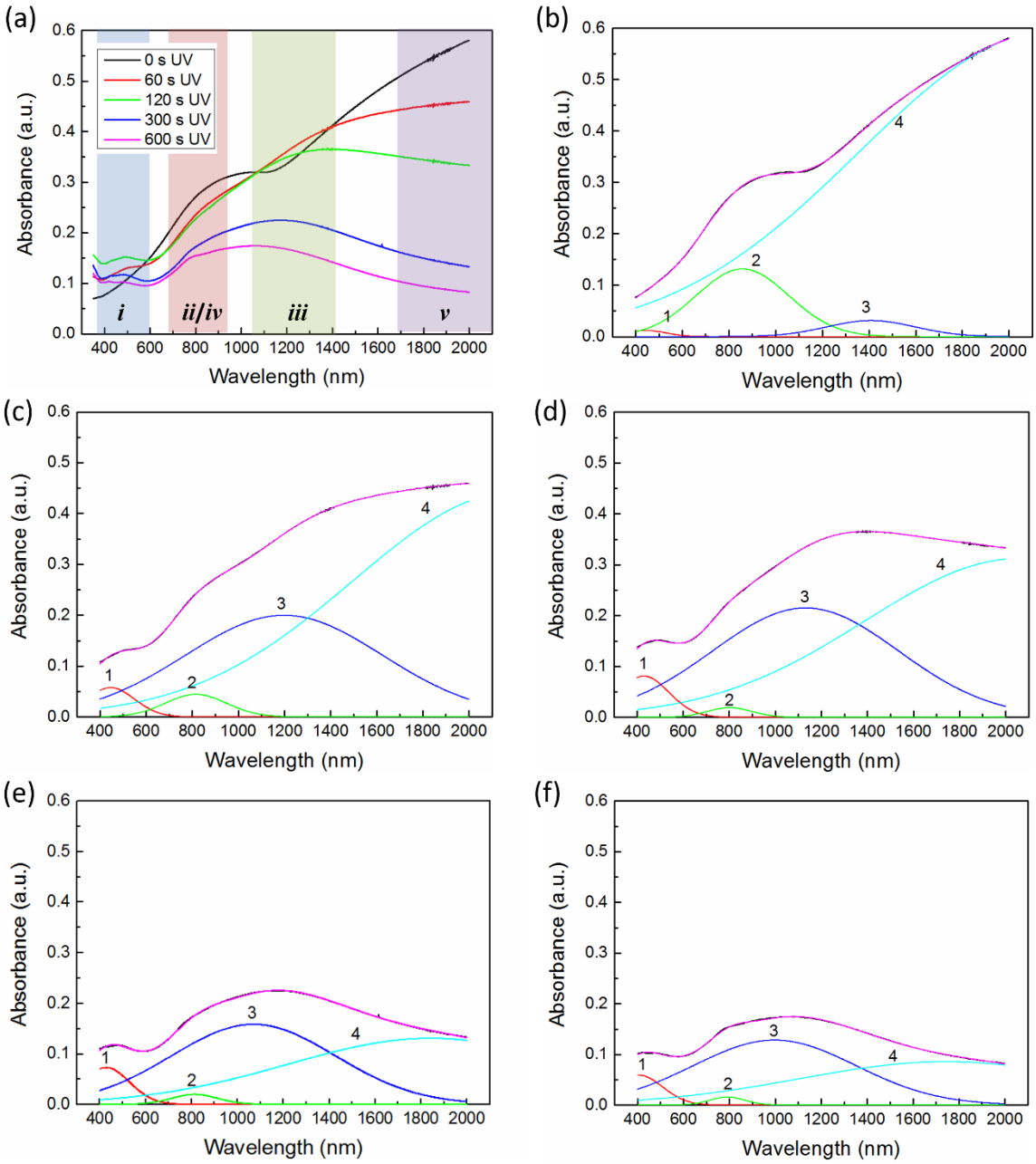

Figure 4. Absorption spectra of samples exposed to UV light for increasing exposure times (a) and deconvolutions of the individual spectra (b-f). b: reference sample, c-f: 60 - 600 s exposure.

3.5 *Impedance spectroscopy*

Impedance spectroscopy was performed on oxidant films exposed to UV light for 0, 120 and 600 seconds with two samples for each exposure time. The impedance was measured in the lateral direction between two gold bottom electrodes. Fig. 5a-b show the real part impedance

and the phase angle of the impedance in the frequency range 100 mHz to 100 kHz. The shape of the phase angle is characteristic for an electrolyte with values close to -90° at high frequencies, approaching 0° at lower frequencies. The impedance close to -90° is purely capacitive and is attributed to dipole relaxation in the electrolyte, whereas the impedance close to 0° is purely resistive and comes from ionic migration.[24] Typically the phase angle goes back to -90° at very low frequencies when a complete double layer is formed on the electrodes. This is however outside the investigated frequency range due to the high impedance values. The ionic resistance can be estimated as the real part of the impedance in the frequency range where the phase angle is close to 0°.[25] In Fig. 5a we can see how the ionic resistance decreases with increasing UV exposure. The resistance (R_{ion}) is inversely proportional to the ion mobility (μ) and the ion concentration (n) in the sample ($R_{ion} \propto 1/[\mu \cdot n]$). A decrease in the resistance thus indicates that the value of at least one of these parameters has increased. An increase in μ could arise from a structural change in the oxidant film and an increase in n means an increase in ionic species, possibly due to a partial dissociation of ionically bound species present in the oxidant (such as the iron and tosylate ions).

Fig. 5c-d show the real part impedance and phase angle of exposed and unexposed samples that were not washed after polymerization. Only one of these samples was baked after polymerization. The unexposed sample shows low impedance and a phase angle indicating purely electronic conductivity while the exposed samples show high impedance and a phase angle that resembles the oxidant solution (Fig. 5b). This means that the charge transport is mainly ionic and the PEDOT has not formed a percolating network in the film. This explains why exposed samples that are not baked after polymerization will dissolve in the washing step. Furthermore, with increasing UV dosage the impedance is reduced and the phase angle becomes more resistive indicating that the conductive network is improving. The exposed and then baked sample has lower impedance than the samples obtained after UV light exposure but

no baking and it has a phase angle that resemble the unexposed sample. This indicates that a conductive network is formed during the baking step.

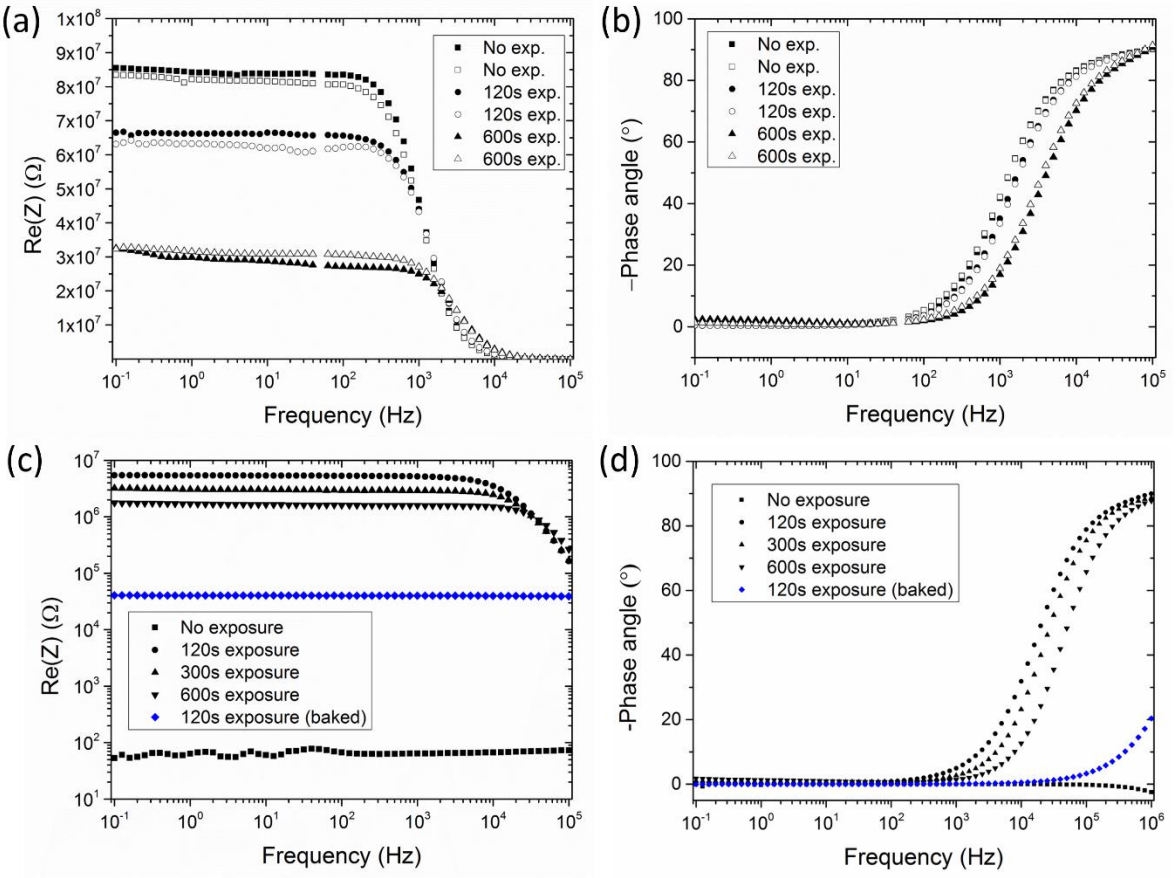

Figure 5. Impedance spectroscopy Bode plots. (a) Real part impedance and (b) phase angle of oxidant films exposed to UV light for increasing time spans. (c) Real part impedance and (d) imaginary part of unwashed samples.

3.6 *XPS and UPS*

The change of the chemical environments in samples exposed to UV light was further investigated by XPS and UPS. Fig. 6a and 6b depicts the S 2p XPS spectra of exposed (300 s) and unexposed PEDOT:Tos. The XPS spectra clearly indicate that there are two kinds of chemical states of sulfur atoms in the pristine and UV exposed PEDOT:Tos. The S 2p signal at the lower binding energy at around 163.6 eV originates from the PEDOT moiety, the feature at higher binding energy at about 167 eV is the contribution from tosylate which is bound to

the oxidized PEDOT. Therefore, the oxidation state of PEDOT:Tos can be extracted from the spectral weight ratio from the two different sulfur states in the film, as explained by Zotti et al.[26] Using the methodology, the oxidation level of the two polymeric films can be determined. By deconvolution of the S 2p spectrum with two sets of S 2p peaks, as shown in Fig. 6 (it should be mentioned that one more set of S 2p at the energy above 168 eV comes from unbound tosylate), the spectral weight of sulfur atoms from PEDOT and negatively charges tosylate molecules can be estimated. As a result, the doping level in unexposed PEDOT:Tos films was 0.23, while the doping level in exposed PEDOT:Tos was 0.16. Another indication of the different doping state of PEDOT is given by the asymmetric tail on the higher binding energy side of the S 2p peak, as the red line shown in Fig. 6a and 6b. The asymmetry is associated with the presence of positive charges on the polymer.[26] The tail in the unexposed samples displays a large asymmetry while it is less pronounced in the exposed sample, which indicates a lower concentration of positive charges in the exposed sample.

Furthermore, the change of the different charge states due to UV exposure in the PEDOT:Tos can also be seen in the UPS measurements, shown in Fig. 6c. There is no obvious change of the work function in the UV exposed samples, but an influence on the valence band feature was observed. There is an enhanced signal in the valence band of the UV exposed PEDOT:Tos film, which can possibly be attributed to the valence feature of neutral PEDOT segments which are more pronounced due to the lower doping level in the exposed samples.

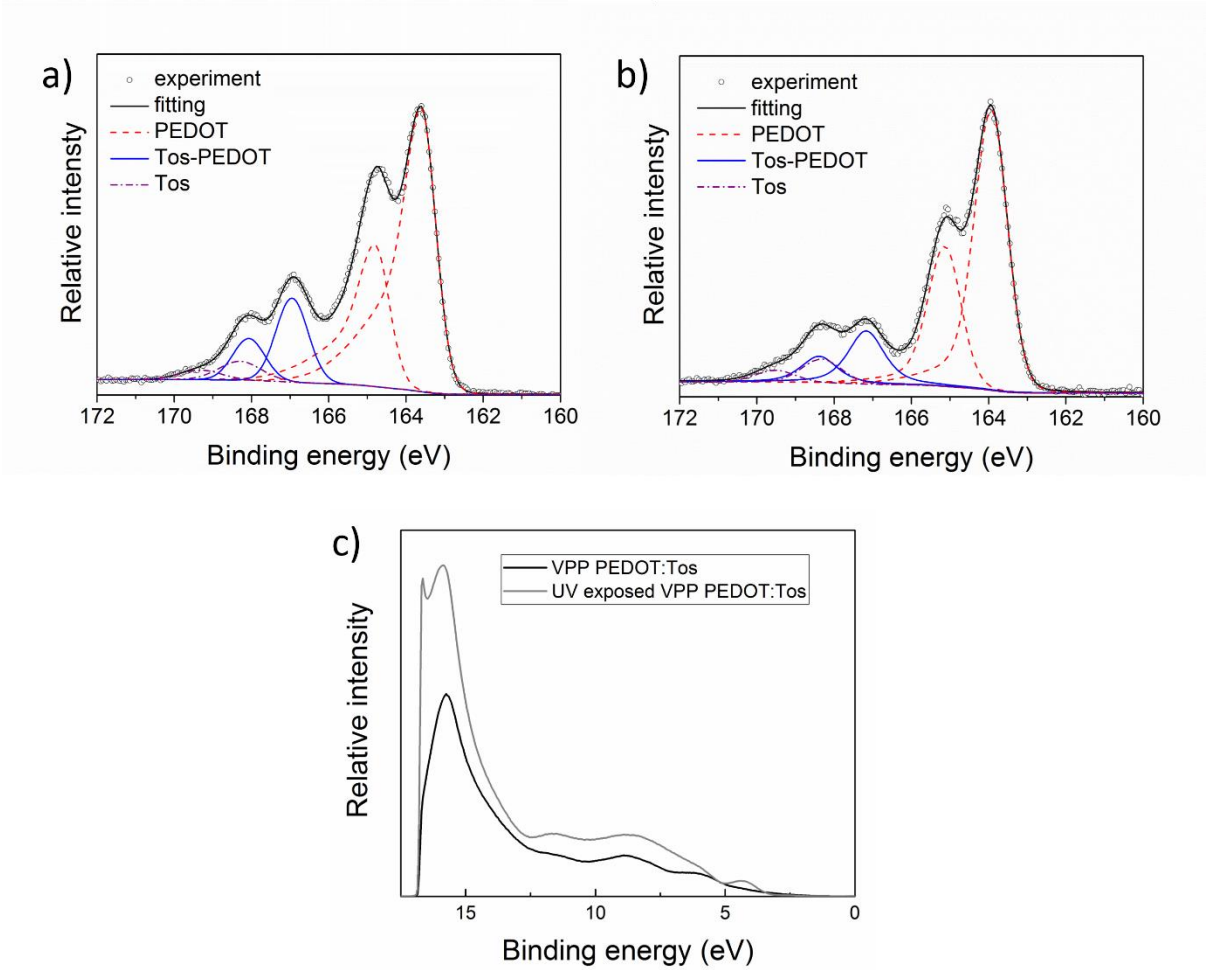

Figure 6. XPS S 2p spectra of exposed (a) and unexposed (b) PEDOT:Tos. The fitting of each S 2p with different components was also presented. (c) The corresponding UPS spectra of exposed (blue line) and unexposed (black line) PEDOT:Tos.

3.7 *GIWAXS*

The exposed (300 s and 600 s UV light) and unexposed polymers were characterized using grazing incidence wide angle X-ray scattering (GIWAXS) to evaluate the effect of UV irradiation on the structuring of the product of the process (Fig. 7). The unexposed sample exhibits good crystallinity and is highly textured, with an "edge-on" orientation, i.e. with lamellar stacking along the surface normal, and the π-stacking in the substrate plane (at Q_{xy}=1.79 $Å^{-1}$). The first three orders of the lamellar peak are clearly distinguished at Q_z = 0.45

$Å^{-1}$ corresponding to a d-spacing of 14 Å. In contrast to the unexposed sample, the exposed samples are amorphous.

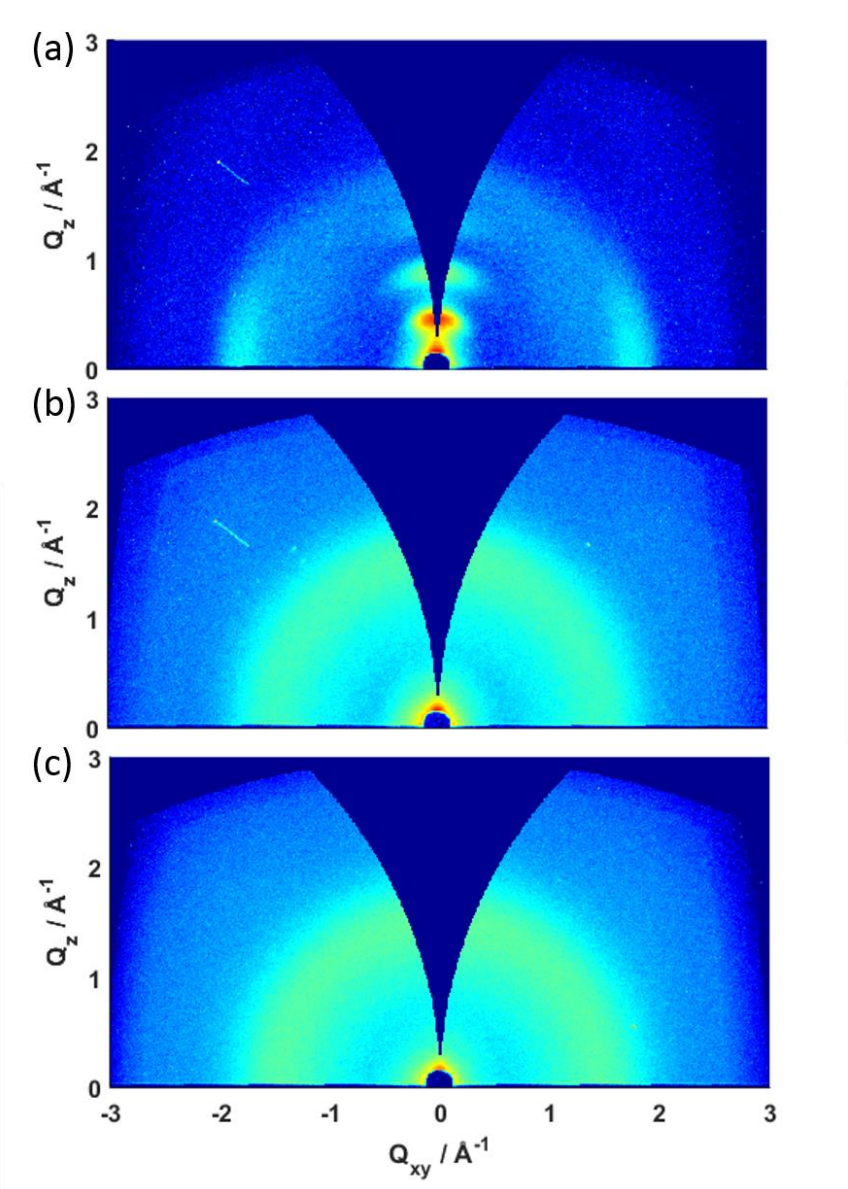

Figure 7. GIWAXS analysis of (a) unexposed PEDOT:Tos and (b-c) PEDOT:Tos obtained after 300 s and 600 s of UV light exposure.

4. DISCUSSION

4.1 *The effect of UV light on the oxidant*

The most notable effect on the polymer produced by the UV light irradiation of the oxidant film is the dramatic change in its electrical conductivity: it spanning over more than 6 orders of magnitude. From the results of FTIR, XPS, UPS, GIWAXS and absorption spectroscopy we know that several factors (such as doping level, polymer chain length and morphology) can explain the conductivity modulation (see section 4.2). Since EDOT VPP is performed after the exposure to UV, a change in the oxidant solution, known to modulate the polymerization reaction kinetics, must be the cause of the change in the electronic and structural properties of the obtained polymeric films. FTIR spectroscopy and impedance spectroscopy of exposed and unexposed oxidant films give some indications of these changes. The most noticeable change in the FTIR spectra of the oxidant solution is the peak at 3400 cm^{-1}. A similar effect has been observed in PEG when irradiated by UV light and has been attributed to photo degradation.[27, 28] The presence of metal ions has been shown to increase the rate of such degradation. However, in our analysis of the bare triblock copolymer we did not see any such effects and the peak at 3400 cm^{-1} appears to originate from the iron-tosylate. The peak indicates an increase in the number of OH-groups that are less strongly h-bonded than the ones that make up the 3115 cm^{-1} band. It is unclear from the FTIR data if the larger freedom in O-H vibrations is related to coordinated water or to the OH-groups in tosylate or both. Irrespective of which, this, together with the larger degree of freedom in the S and O atoms as well as in the S-C bonds indicates a change in the coordination between iron, tosylate and water. Such a change in coordination could also explain the reduction in ionic resistance upon UV light exposure. Indeed, a reduced coordination could result in a decrease in the screening of charges and thus in an effective increase in the concentration of mobile ions. Alternatively, a change in the coordination of water could affect the ionic mobility of the oxidant, since water present in an

electrolyte largely affects the ion mobility, which in turn would affect the ionic resistance. Furthermore, previous investigations have shown that small changes in the amount of coordinated water in the oxidant solution can have a large impact on the VPP process.[29, 30] Mobility of the oxidant is important to the VPP process, given the requirement for transport of these ions to the liquid-vapor interface to facilitate further polymerization to occur.[31, 32]

Changes in the coordination between iron, tosylate and water have been shown to have large effects on the polymerization kinetics. Hojati-Talemi et al. demonstrated how a change in the coordination shell of iron could be achieved by the addition of aprotic polar solvents and chelating ligands, leading to a change in the number of nucleation sites and thus influencing the polymerization rate.[33] A large number of nucleation sites is associated with faster polymerization rates and smaller polymer grains which in turn leads to poor conductivity and more fragile films. A high effective reactivity of the oxidant in chemical polymerization has been associated with poor film quality and low conductivity. For this reason, chemicals that suppress the reactivity, such as pyridine which is a weak base, are often added to the oxidant solution to achieve a more controlled polymerization and thus to films with high conductivity.[34] Furthermore, faster polymerization reactions explain why the thickness of films polymerized for the same time increases linearly with UV light exposure time.

4.2 *Effects of UV light on the polymer*

The dramatic drop in conductivity of PEDOT:Tos upon UV light irradiation of the oxidant films can be explained by several factors such as shorter conjugation length, lower doping state, shorter polymer chains and structural disorder. From GIWAXS measurements we know that the exposed polymer is highly disordered (see section 3.7). The charge transport in conductive polymers is mainly limited by charge hopping which depends on the π-π coupling between polymer chains and is strongly affected by the microscopic order. This suggests that the disorder is a major contributor to the reduction in conductivity. However, a structural change

alone cannot account for the change in the optical properties shown by absorption spectroscopy (see section 3.4). The absorption spectra of conductive polymers are largely dependent on the concentration of charge carriers. From our FTIR analyses we can see that the concentration of charge carriers has been reduced (see section 3.3). Besides the deconvolution of the XPS spectra indicated a reduced doping state (see section 3.6). Also, the deconvolution of the absorption spectra of polymers exposed for different time periods suggests a gradual transition from bipolarons to polarons as the major charge carrier. The spectra also reveal an unusually large band gap energy of the neutral polymer. Such a shift in energy could be an indication of a shortening of the polymer chains and/or the conjugation length. Apperloo et al. investigated the absorption spectra of EDOT oligomers with phenyl side groups.[35] In their work, the wavelength at the maximum absorbance of EDOT dimers and trimers are in good agreement with the wavelength of the neutral chain absorbance peak in exposed PEDOT:Tos. This theory is also corroborated by the increase in C-C-H stretching modes and decrease in C=C stretching modes observed in FTIR measurements.[21] In section 4.1 we hypothesized that a change in the coordination of the oxidant upon UV irradiation could lead to an increased effective reactivity and faster polymerization rates. Interestingly, a strong oxidant and fast polymerization kinetics has previously been linked to the formation of short oligomers with broken conjugation.[34, 36]

The observation that the exposed films dissolve in ethanol upon washing unless it is baked after polymerization could be explained both by the poor crystallinity and by the proposed shortening in polymer chains. Both effects could lead to poor inter-chain entanglement and fragile films. This theory is validated by the results in section 3.5 where it was shown that a continuous polymer network is not formed within the oxidant solution unless the sample is baked after polymerization. After 30 minutes of polymerization, all the oxidant has not been consumed and hence there will be unreacted EDOT monomers adsorbed within or adsorbed onto the film. When the sample is put on the hotplate in the post polymerization baking step

the high temperature initiates a rapid chemical polymerization of the residual unreacted EDOT. The films obtained with the included baking step are thicker than those without it. The additional polymer formed during this step could explain why the films survive the washing step. In a similar manner to the baked samples, films that were polymerized for 15 hours were thicker than those produced during the 30-minute polymerization time, and no further increase in their thickness or change the conductivity of the films were measured upon baking them after the polymerization. This results suggests that all the oxidant had been consumed.

5. CONCLUSIONS

In this work we have demonstrated a novel technique to pattern the conductive polymer PEDOT:Tos produced by VPP. By exposing the oxidant solution to UV light through a photomask prior to polymerization we have shown that it is possible to locally modulate the conductivity of the resulting polymer film over 6 orders of magnitude as well as selectively removing parts of the film. We explored the patterning mechanism and the resulting polymer films. We hypothesize that the UV light changes Fe(III) coordination shell in the oxidant solution leading to faster polymerization kinetics. This faster kinetics results in the synthesis of short polymer chains with different electronic structure and morphology compared to the PEDOT produced without the UV light exposure step. These changes affect both the electrical and optical properties of the polymer.

This technique combines the functionality of both conventional photolithography of conductive polymers that yields a step-like profile of the pattern, and local chemical or electrochemical over-oxidation of PEDOT that produces a continuous film with regions of different conductivity. However, while the over-oxidation technique will result in the same conductivity

in all exposed regions, the method presented in this work can produce regions of different conductivity within the same film. This technique even allows for the possibility to produce gradients in conductivity, something that would be difficult to achieve with other patterning methods. The method also involves fewer processing steps than conventional photolithography and is not dependent on any photoresist or developers. Also, since a number of conductive polymers can be produced by VPP using the same oxidant by adding different monomers, their patterning through the developed technique can be envisioned.

The resolution of the patterning technique is currently limited to ~10 μm because of the difficulty of putting the photomask close to the substrate in proximity patterning. Contact patterning, which is necessary for high resolution, is not possible because the mask sticks to the oxidant film. A reformulation of the oxidant recipe or optimization of other processing parameters that would make contact patterning possible could further increase resolution to the same level as conventional photolithography.

A number of unique device applications could be realized by the patterning technique spanning from resistor networks with conductivities varying over 6 orders of magnitude to electrochromic displays and sensors.

ACKNOWLEDGEMENTS

The research was funded by the Knut and Alice Wallenberg Foundation; Power Paper project (KAW 2011.0050), Tail of the Sun (KAW 2014.0041) and a scholar grant (KAW 2012.0302). The authors wish to thank professor Olle Inganäs and professor Mats Fahlman at Linköping University for access to equipment in their facilities.

REFERENCES

[1] M. V. Fabretto, D. R. Evans, M. Mueller, K. Zuber, P. Hojati-Talemi, R. D. Short, et al., Chemistry of Materials 2012, 24, 3998-4003.

[2] B. Cho, K. S. Park, J. Baek, H. S. Oh, Y.-E. Koo Lee, M. M. Sung, Nano Letters 2014, 14, 3321-7.

[3] S.-F. Tseng, W.-T. Hsiao, K.-C. Huang, D. Chiang, Applied Physics A 2012, 112, 41-7.

[4] E. B. Secor, P. L. Prabhumirashi, K. Puntambekar, M. L. Geier, M. C. Hersam, The Journal of Physical Chemistry Letters 2013, 4, 1347-51.

[5] B. Winther-Jensen, F. C. Krebs, Solar Energy Materials and Solar Cells 2006, 90, 123-32.

[6] H. J. Lee, T. H. Park, J. H. Choi, E. H. Song, S. J. Shin, H. Kim, et al., Organic Electronics: physics, materials, applications 2013, 14, 416-22.

[7] D. S. Leem, P. H. Wöbkenberg, J. Huang, T. D. Anthopoulos, D. D. C. Bradley, J. C. De Mello, Organic Electronics: physics, materials, applications 2010, 11, 1307-12.

[8] J. Huang, R. Xia, Y. Kim, X. Wang, J. Dane, O. Hofmann, et al., Journal of Materials Chemistry 2007, 17, 1043-9.

[9] P. G. Taylor, J. K. Lee, A. A. Zakhidov, M. Chatzichristidi, H. H. Fong, J. A. DeFranco, et al., Advanced Materials 2009, 21, 2314-7.

[10] S. Ouyang, Y. Xie, D. Wang, D. Zhu, X. Xu, T. Tan, et al., Journal of Polymer Science, Part B: Polymer Physics 2014, 52, 1221-6.

[11] J. A. Defranco, B. S. Schmidt, M. Lipson, G. G. Malliaras, Organic Electronics: physics, materials, applications 2006, 7, 22-8.

[12] C. D. O'Connell, M. J. Higgins, H. Nakashima, S. E. Moulton, G. G. Wallace, Langmuir 2012, 28, 9953-60.

[13] J. Kim, J. You, E. Kim, Macromolecules 2010, 43, 2322-7.

[14] P. Tehrani, N. D. Robinson, T. Kugler, T. Remonen, L. O. Hennerdal, J. Häll, et al., Smart Materials and Structures 2005, 14, N21-N5.

[15] D. Apitz, R. P. Bertram, N. Benter, W. Hieringer, J. W. Andreasen, M. M. Nielsen, et al., Physical Review E 2005, 72, 036610.

[16] K. Van De Ruit, I. Katsouras, D. Bollen, T. Van Mol, R. A. J. Janssen, D. M. De Leeuw, et al., Advanced Functional Materials 2013, 23, 5787-93.

[17] A. Laforgue, L. Robitaille, Macromolecules 2010, 43, 4194-200.

[18] Useful Reagents and Ligands. Inorganic Syntheses: John Wiley & Sons, Inc.; 2002. p. 75-121.

[19] H. Kuzmany, N. S. Sariciftci, H. Neugebauer, A. Neckel, Physical Review Letters 1988, 60, 212-5.

[20] C. Kvarnström, H. Neugebauer, A. Ivaska, N. S. Sariciftci, Journal of Molecular Structure 2000, 521, 271-7.

[21] S. G. Im, K. K. Gleason, Macromolecules 2007, 40, 6552-6.

[22] P. Pelikán, M. Čeppan, M. Liška. Applications of numerical methods in molecular spectroscopy. Boca Raton: CRC Press; 1994. 341 p. p.
[23] O. Bubnova, Z. U. Khan, A. Malti, S. Braun, M. Fahlman, M. Berggren, et al., Nature Materials 2011, 10, 429-33.
[24] O. Larsson, E. Said, M. Berggren, X. Crispin, Advanced Functional Materials 2009, 19, 3334-41.
[25] X. Qian, N. Gu, Z. Cheng, X. Yang, E. Wang, S. Dong, Journal of Solid State Electrochemistry 2001, 6, 8-15.
[26] G. Zotti, S. Zecchin, G. Schiavon, F. Louwet, L. Groenendaal, X. Crispin, et al., Macromolecules 2003, 36, 3337-44.
[27] H. Kaczmarek, A. Sionkowska, A. Kamińska, J. Kowalonek, M. Świątek, A. Szalla, Polymer Degradation and Stability 2001, 73, 437-41.
[28] J. F. Rabek, L. Å. Lindén, H. Kaczmarek, B. J. Qu, W. F. Shi, Polymer Degradation and Stability 1992, 37, 33-40.
[29] M. Fabretto, K. Zuber, C. Hall, P. Murphy, H. J. Griesser, Journal of Materials Chemistry 2009, 19, 7871-8.
[30] M. Mueller, M. Fabretto, D. Evans, P. Hojati-Talemi, C. Gruber, P. Murphy, Polymer 2012, 53, 2146-51.
[31] R. Brooke, M. Fabretto, P. Hojati-Talemi, P. Murphy, D. Evans, Polymer 2014, 55, 3458-60.
[32] D. Evans, M. Fabretto, M. Mueller, K. Zuber, R. Short, P. J. Murphy, Journal of Materials Chemistry 2012, 22, 14889-95.
[33] P. Hojati-Talemi, C. Bächler, M. Fabretto, P. Murphy, D. Evans, ACS Applied Materials and Interfaces 2013, 5, 11654-60.
[34] J. P. Lock, S. G. Im, K. K. Gleason, Macromolecules 2006, 39, 5326-9.
[35] J. J. Apperloo, L. B. Groenendaal, H. Verheyen, M. Jayakannan, R. A. J. Janssen, A. Dkhissi, et al., Chemistry – A European Journal 2002, 8, 2384-96.
[36] S. Sadki, P. Schottland, N. Brodie, G. Sabouraud, Chemical Society Reviews 2000, 29, 283-93.

Supplementary information for

Patterning and Conductivity Modulation of Conductive Polymers by UV Light Exposure

Jesper Edberg[a], Donata Iandolo[a], Robert Brooke[a], Xianjie Liu[b], Chiara Musumeci[b], Jens Wenzel Andreasen[c], Daniel T. Simon[a], Drew Evans[d], Isak Engquist[a*] and Magnus Berggren[a]

*Corresponding author: isak.engquist@liu.se

[a]Linköping University

Department of Science and Technology, Laboratory of Organic Electronics

SE-601 74 Norrköping, Sweden

[b]Linköping University

Department of Physics, Chemistry and Biology

SE-581 83 Linköping, Sweden

[c]Technical University of Denmark

Department of Energy Conversion and Storage

4000 Roskilde, Denmark

[d]University of South Australia

Future Industries Institute

5001 Adelaide, Australia

This document includes:

Supplementary text

Figures S1-S6

Two patterning routes:

Fig. S1a shows a schematic picture of the two patterning routes that can either be used to remove the regions that were exposed to UV light during the patterning step or to keep these low-conductivity regions. Fig. S1a and S1b show microscope images of PEDOT-patterns

where one sample (S1b) was baked after polymerization while the other (S1c) was not baked. The sample was patterned on gold-coated glass substrates to give the patterns better optical contrast. In Fig. S1c, the polymer between the patterns has been completely removed. We can see that both patterning routes produces high resolution patterns.

Fig. S2 shows the different steps of removing the polymer in the exposed regions in a sample where the oxidant was patterned prior to polymerization. Fig. S2a shows the sample directly after taking it out of the polymerization chamber. The sample is then put in ethanol where the exposed regions start to dissolve (Fig. S2b). Fig. S2c shows the sample after drying and Fig. 2 shows the sample under a light source.

AFM and conductive AFM (C-AFM):

Atomic force microscopy measurements were performed on unexposed samples of PEDOT:Tos and on samples where the oxidant was exposed to UV light for 600 s before polymerization. Fig. S3 shows the height data of the unexposed (Fig. S3a) and the exposed (Fig. S3b) samples. In the unexposed sample the surface roughness is ~40 nm while the exposed sample have a roughness of 200-300 nm. The unexposed sample is thus much flatter than the exposed sample.

Conductive AFM (C-AFM) measurements were performed in the out-of-plane direction on PEDOT:Tos samples produced on gold-coated glass substrates. A photomask was used to pattern lines with different widths in the polymer. The patterns are the same as shown in Fig. 2e and 2f where the narrow lines are the regions that were protected from UV by the mask. Fig. S4 shows the result of C-AFM on lines with 10 µm, 20 µm, 50 µm and 100 µm width. For the 100 µm wide sample only the edge of the line is shown. The lines are centered where the current is peaking and the height is lowest.

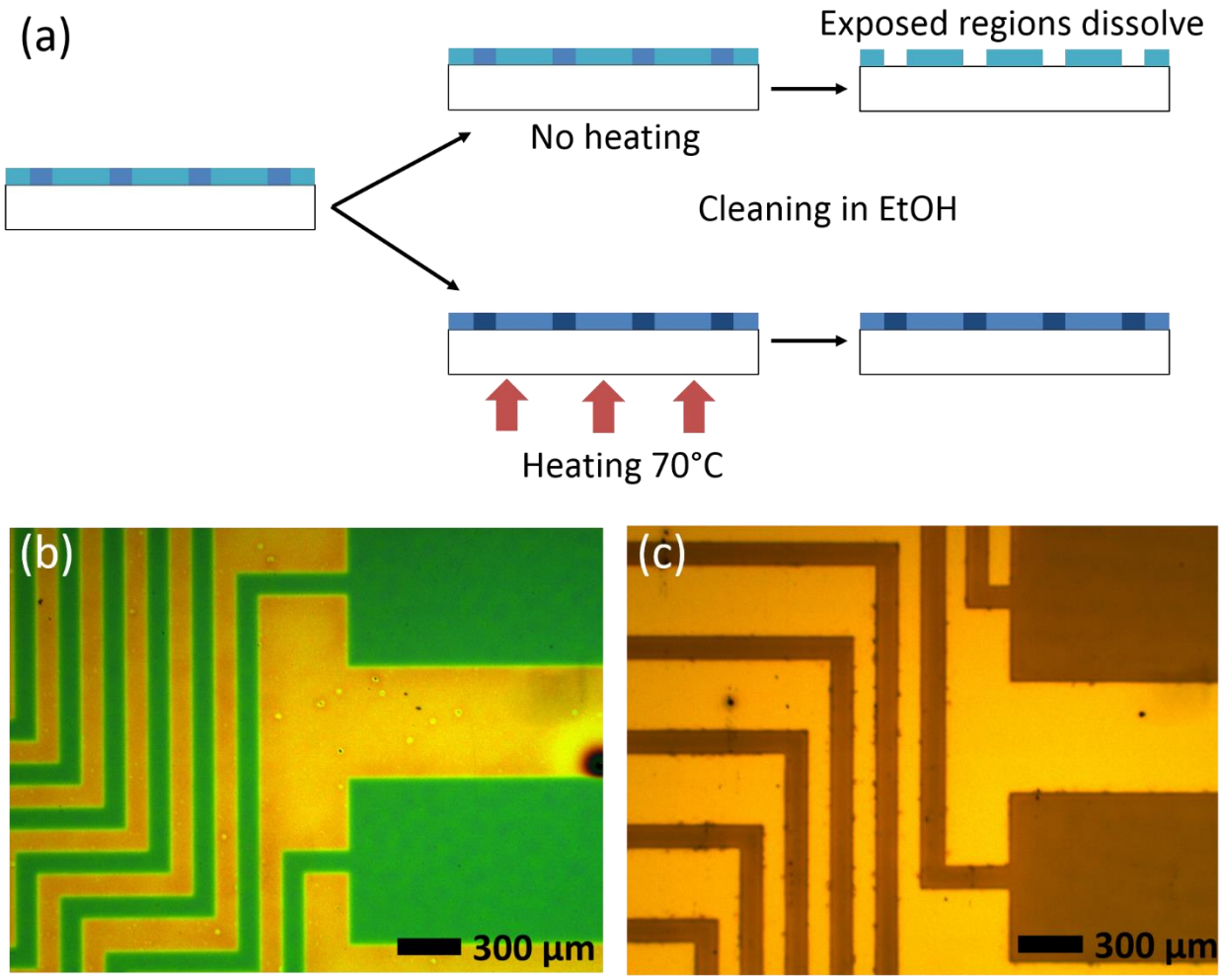

Figure S1. Schematic picture of the two patterning routes (a) and two patterned samples on gold substrates where one sample (b) was baked after polymerization while the other (c) was not baked.

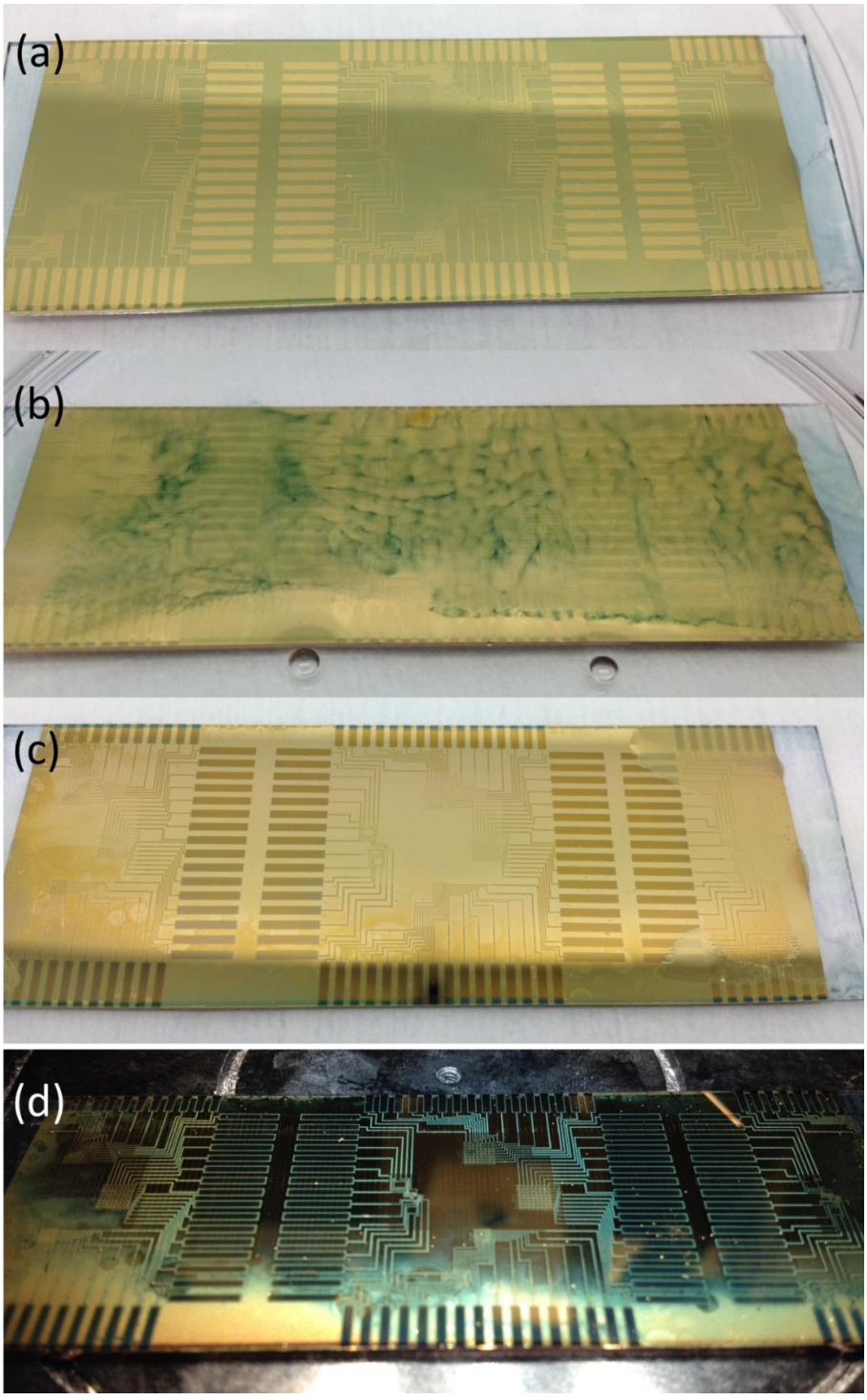

Figure S2. The sequential steps to remove exposed regions after polymerization in a PEDOT-pattern on gold substrate.

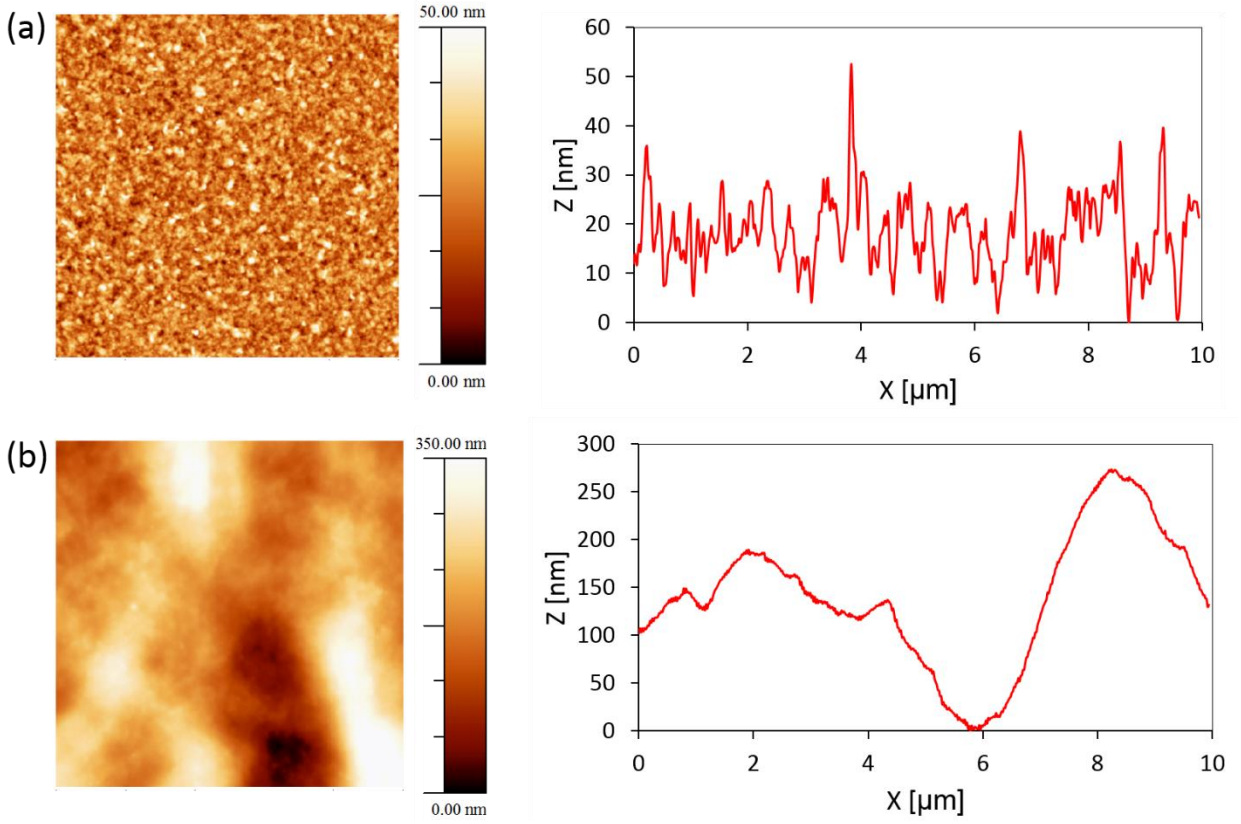

Figure S3. AFM images (left) and height data (right) of unexposed PEDOT (a) and PEDOT where the oxidant was exposed to UV light for 600 s (b).

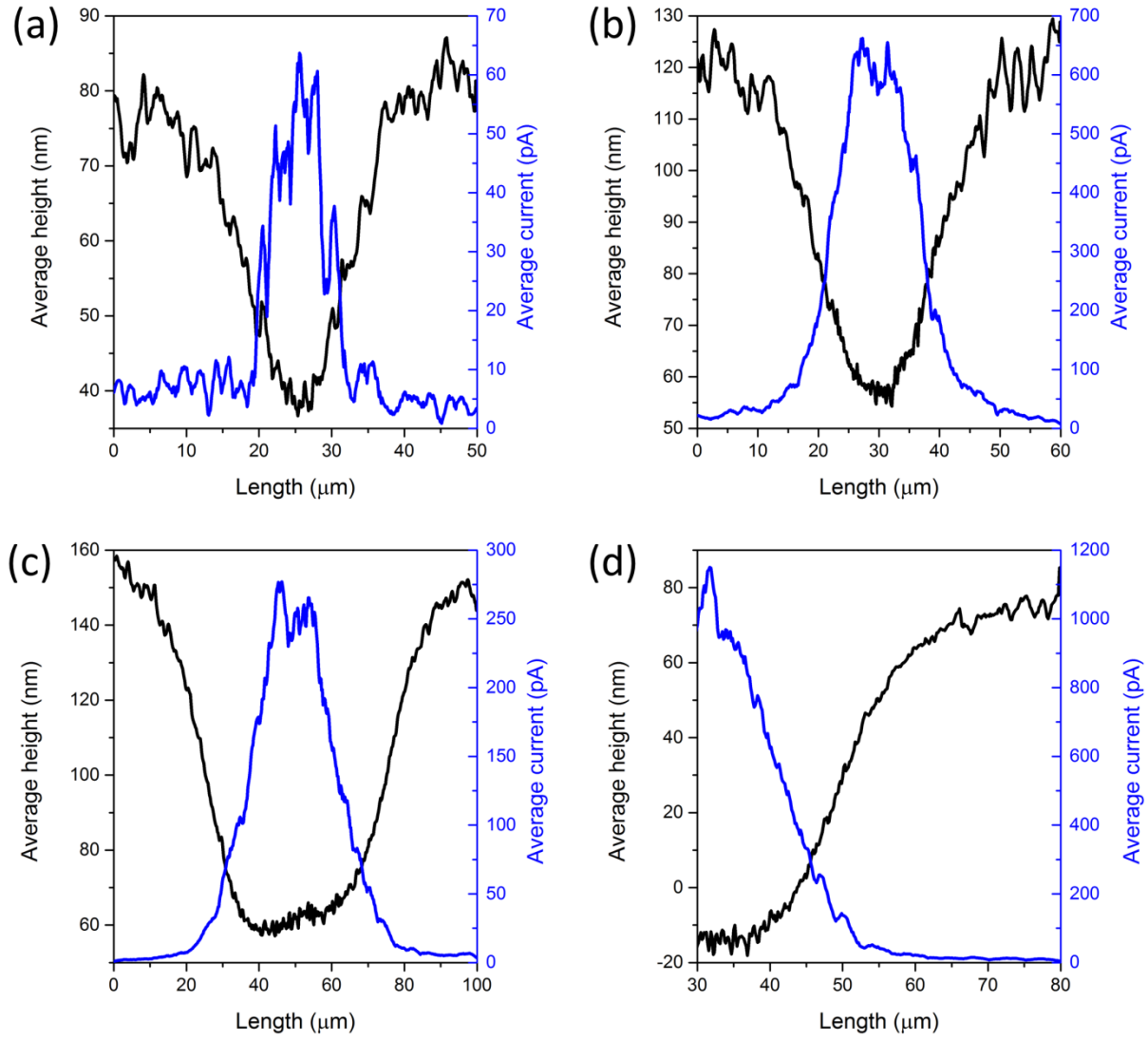

Figure S4. Conductive AFM measurements of (a) 10 µm, (b) 20 µm, (c) 50 µm and (d) 100 µm wide PEDOT-lines patterned on gold-coated glass substrates. (Only a part of the 100 µm line is shown.)

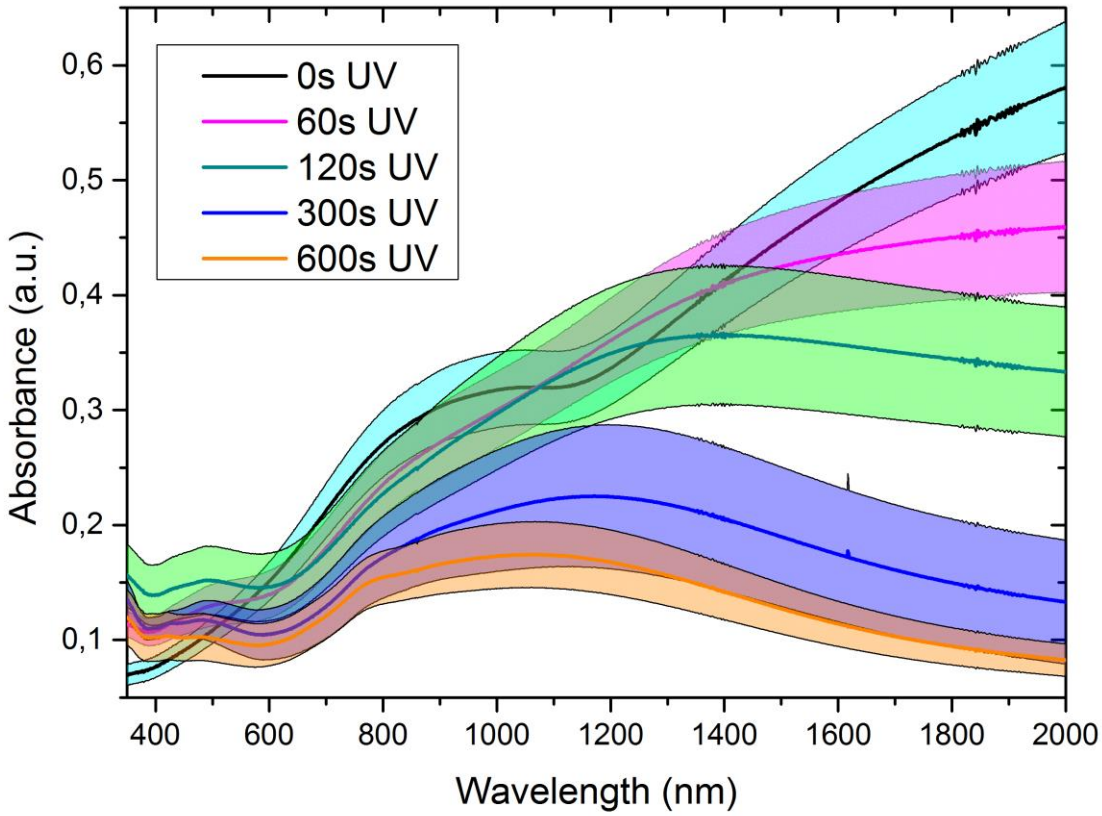

Figure S5. UV-Vis-NIR absorption spectra with error bars of PEDOT:Tos films exposed to different UV light doses.

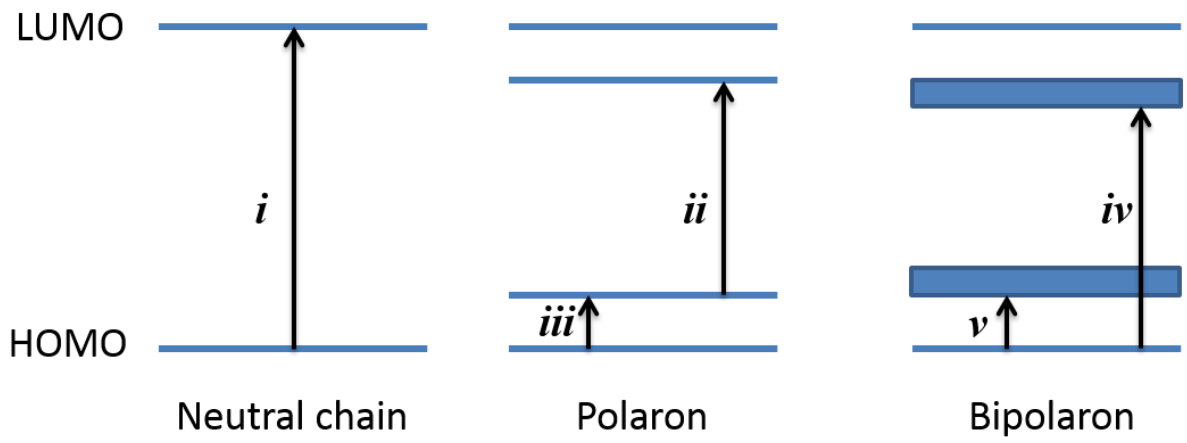

Figure S6. Main electronic transitions related to the optical absorption in PEDOT:Tos (adapted from Bubnova et al.[1]).

REFERENCES

[1] O. Bubnova, Z. U. Khan, A. Malti, S. Braun, M. Fahlman, M. Berggren, et al., Nature Materials 2011, 10, 429-33.